Biochemistry and Biophysics Reports 2 (2015) 36–44

Contents lists available at ScienceDirect

Biochemistry and Biophysics Reports

journal homepage: www.elsevier.com/locate/bbrep

Interplay of catalytic subsite residues in the positioning of α-D-glucose 1-phosphate in sucrose phosphorylase

Patricia Wildberger [a], Gaia A. Aish [b], David L. Jakeman [b], Lothar Brecker [c], Bernd Nidetzky [a,d,*]

[a] Institute of Biotechnology and Biochemical Engineering, Graz University of Technology, NAWI Graz, Petersgasse 12, A-8010 Graz, Austria
[b] College of Pharmacy, Dalhousie University, PO Box 15,000, 5968 College Street, Halifax, Nova Scotia, Canada B3H 4R2
[c] Institute of Organic Chemistry, University of Vienna, Währingerstraße 38, A-1090 Vienna, Austria
[d] Austrian Centre of Industrial Biotechnology, Petersgasse 14, A-8010 Graz, Austria

ARTICLE INFO

Article history:
Received 15 February 2015
Received in revised form
30 March 2015
Accepted 1 April 2015
Available online 17 April 2015

Keywords:
Sucrose phosphorylase
Glycoside hydrolase family GH-13
Catalytic subsite
α-D-Glucose 1-phosphate
Molecular docking
Binding recognition

ABSTRACT

Kinetic and molecular docking studies were performed to characterize the binding of α-D-glucose 1-phosphate (αGlc 1-*P*) at the catalytic subsite of a family GH-13 sucrose phosphorylase (from *L. mesenteroides*) in wild-type and mutated form. The best-fit binding mode of αGlc 1-*P* dianion had the phosphate group placed *anti* relative to the glucosyl moiety (adopting a relaxed $^4C_1$ chair conformation) and was stabilized mainly by hydrogen bonds from residues of the enzyme's catalytic triad (Asp^{196}, Glu^{237} and Asp^{295}) and from Arg^{137}. Additional feature of the αGlc 1-*P* docking pose was an intramolecular hydrogen bond (2.7 Å) between the glucosyl C2-hydroxyl and the phosphate oxygen. An inactive phosphonate analog of αGlc 1-*P* did not show binding to sucrose phosphorylase in different experimental assays (saturation transfer difference NMR, steady-state reversible inhibition), consistent with evidence from molecular docking study that also suggested a completely different and strongly disfavored binding mode of the analog as compared to αGlc 1-*P*. Molecular docking results also support kinetic data in showing that mutation of Phe^{52}, a key residue at the catalytic subsite involved in transition state stabilization, had little effect on the ground-state binding of αGlc 1-*P* by the phosphorylase. However, when combined with a second mutation involving one of the catalytic triad residues, the mutation of Phe^{52} by Ala caused complete (F52A_D196A; F52A_E237A) or very large (F52A_D295A) disruption of the proposed productive binding mode of αGlc 1-*P* with consequent effects on the enzyme activity. Effects of positioning of αGlc 1-*P* for efficient glucosyl transfer from phosphate to the catalytic nucleophile of the enzyme (Asp^{196}) are suggested. High similarity between the αGlc 1-*P* conformers bound to sucrose phosphorylase (modeled) and the structurally and mechanistically unrelated maltodextrin phosphorylase (experimental) is revealed.
© 2015 The Authors. Published by Elsevier B.V. This is an open access article under the CC BY-NC-ND license (http://creativecommons.org/licenses/by-nc-nd/4.0/).

1. Introduction

Sucrose phosphorylase catalyzes the conversion of sucrose and phosphate into α-D-glucose 1-phosphate (αGlc 1-*P*) and D-fructose [1,2]. The enzyme belongs to a large family of glycoside hydrolases and transglycosylases (family GH-13) that act on α-glucosidic oligosaccharide and polysaccharide substrates [3,4]. Sucrose phosphorylase presents a unique enzymatic reactivity within family GH-13 (EC 2.4.1.7) that involves utilization of phosphate as the glucosyl acceptor substrate. Mechanistically, as in other enzymes of family GH-13 [4], reaction occurs through a double displacement-like catalytic process that implicates a covalent β-glucosyl enzyme intermediate and therefore proceeds with retention of α-anomeric configuration in the transferred D-glucosyl residue [2,5]. The active-site of sucrose phosphorylase consists of a highly conserved Asp/Glu/Asp triad of residues that fulfill key roles in catalysis, as shown in Scheme 1 [2,5–10]. An aromatic residue, a phenylalanine, is also present (Fig. 1) and a catalytic function has only recently been proposed: the π electron cloud of the phenyl sidechain provides selective stabilization of the glucosyl oxocarbenium ion-like species formed in each transition state of the reaction [11]. The aromatic residue is highly conserved among glycoside hydrolases of family GH-13, as pointed out by Wildberger et al. [11], and it is either a Phe or a Tyr. Its function in catalysis is likely to be also conserved across the large family GH-13.

The catalytic reaction pathway of sucrose phosphorylase is identical to those of other sucrose-converting enzymes in family

Abbreviations: αGlc 1-*P*, α-D-glucose 1-phosphate; SPase, sucrose phosphorylase; *Lm*SPase, SPase from *Leuconostoc mesenteroides*

* Corresponding author at: Institute of Biotechnology and Biochemical Engineering, Graz University of Technology, NAWI Graz, Petersgasse 12, A-8010 Graz, Austria. Tel.: +43 316 873 8400; fax: +43 316 873 8434.
E-mail address: bernd.nidetzky@tugraz.at (B. Nidetzky).

http://dx.doi.org/10.1016/j.bbrep.2015.04.001
2405-5808/© 2015 The Authors. Published by Elsevier B.V. This is an open access article under the CC BY-NC-ND license (http://creativecommons.org/licenses/by-nc-nd/4.0/).

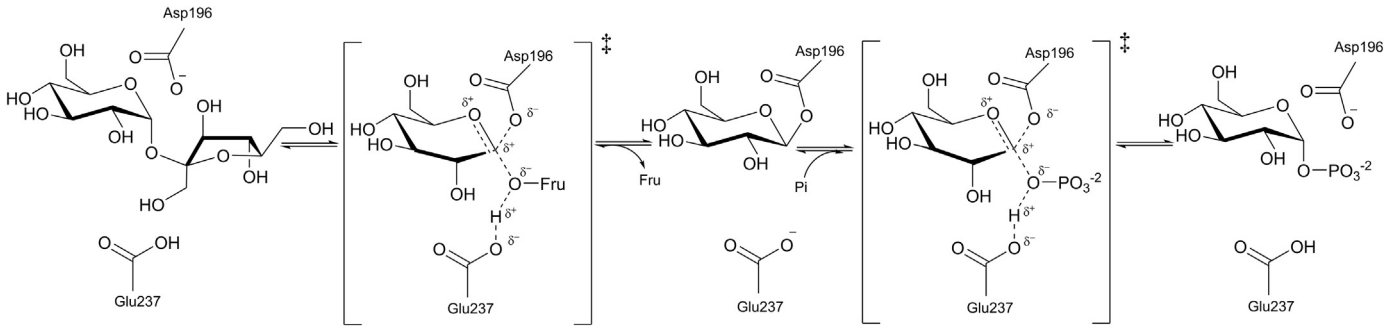

Scheme 1. Catalytic reaction of sucrose phosphorylase proceeds in two steps via a covalent glucosyl-enzyme intermediate. In the enzyme's active-site, Asp^{196} (LmSPase numbering) is the catalytic nucleophile, and Glu^{237} is the catalytic acid–base. Not shown is Asp^{295} that facilitates the reaction through hydrogen bonding interactions with the 2-OH, thus contributing to substrate positioning and transition state stabilization. Also not shown is the conserved Phe^{52} which is additionally important for transition state stabilization (see Fig. 1).

GH-13 [12–14] up to the level of the covalent intermediate (*enzyme glucosylation*), but diverges from them in the subsequent step of *enzyme deglucosylation* where phosphate acts as the incoming nucleophile and αGlc 1-*P* is released as final product of the overall enzymatic transglucosylation (Scheme 1). To understand how the conserved active-site groups of a family GH-13 glycoside hydrolase accommodate the catalytic function of a phosphorylase presents an interesting problem of mechanistic enzymology. A previous study has shown that glucosyl transfer from the catalytic nucleophile of sucrose phosphorylase (from *Leuconostoc mesenteroides*; Asp^{196}) to phosphate is readily reversible with an equilibrium constant of 2.89 (30 °C, pH 7.0) [11]. Another study showed that, unlike enzyme glucosylation from sucrose where catalytic assistance from Glu^{237} as Brønsted acid is critical to promote the reaction (Scheme 1), enzyme deglucosylation to phosphate takes place efficiently despite mutation of Glu^{237} into a glutamine and irrespective of the protonation state of the original glutamic acid's sidechain [7]. A number of studies show that reaction of sucrose phosphorylase in the backwards direction has high relevance for carbohydrate synthesis, allowing a variety of α-D-glucosides to be prepared efficiently from αGlc 1-*P* as the donor substrate [15–18].

In this paper, we would like to present evidence from kinetic and molecular docking experiments that were designed to examine two central problems of the catalytic half-reaction of sucrose phosphorylase with αGlc 1-*P*. Firstly, how is αGlc 1-*P* positioned at the active-site of the enzyme? Crystal structures of sucrose phosphorylase (from *Bifidobacterium adolescentis*) in apo-form [6] and in a form bound with D-glucose [5] have been determined. A structure of the β-glucosyl enzyme intermediate has also been determined [5], and a sucrose-bound enzyme structure has been obtained of an enzyme variant in which the catalytic glutamic acid had been replaced by glutamine [5]. However, no enzyme structure bound with αGlc 1-*P* exists and there have only been limited efforts to characterize the binding of αGlc 1-*P* with modeling techniques. We show here that in the best-fit binding mode obtained from molecular docking studies, the αGlc 1-*P* dianion had the phosphate group placed *anti* relative to the glucosyl moiety which in turn adopted a relaxed $^4C_1$ chair conformation (Fig. 1). Bound αGlc 1-*P* was stabilized mainly by hydrogen bonds from residues of the enzyme's catalytic triad and from an additional arginine that created a phosphate recognition site. Another distinct feature of the αGlc 1-*P* docking pose was an intramolecular hydrogen bond (2.7 Å distance) between the glucosyl C2-hydroxyl and the phosphate oxygen. The modeled sucrose phosphorylase-bound conformer of αGlc 1-*P* was almost identical to the αGlc 1-*P* conformer observed previously in the crystal structure of maltodextrin phosphorylase (from *Escherichia coli*) [19]. This result was interesting because the interactions involved in substrate binding recognition as well as the catalytic mechanisms are completely different in the two enzymes. Maltodextrin phosphorylase is a member of the glycosyltransferase family GT-35. We also show that a close structural but inactive analog of αGlc 1-*P*, D-glucose 1-methylene phosphonate [20,21], does not bind to sucrose phosphorylase.

The second mechanistic problem examined herein was the interplay between the active-site phenylalanine and residues of the catalytic triad in positioning the αGlc 1-*P* for catalysis. Besides molecular docking studies, we created three double mutants of *L. mesenteroides* sucrose phosphorylase in which the Phe^{52} and one of the triad residues had been substituted, each by alanine. The prominent and highly conserved position of the Phe in the active-site of the phosphorylase (Fig. 1) justified selection of this residue as prime target for mutagenesis. Note however that the interest here was on the effect of *combined substitution* of Phe^{52} and another residue from the catalytic triad (Asp^{196}, Glu^{237}, Asp^{295}). Consequences of each double residue replacement were analyzed in kinetic experiments, and a complete free-energy of F52A_D295A mutant was derived from the data. We provide evidence that Phe^{52} is essential for effective substrate binding and catalytic function of the sucrose phosphorylase active-site. Considering the high degree of conservation of active-site residues in members of family GH-13, the results have relevance not only for sucrose phosphorylases but also in a family-wide context.

2. Materials and methods

2.1. Chemicals and reagents

Pfu DNA polymerase was from Promega (Madison, USA). DpnI was from Fermentas (Burlington, Canada). Oligonucleotides were from Invitrogen (Carlsbad, USA). DNA sequencing was performed at LGC Genomics (Berlin, Germany). The plasmid vector *p*ASK-IBA7+, anhydrotetracycline and all materials used for *Strep*-tag purification were from IBA (Göttingen, Germany). Fractogel EMD-DEAE column (diameter: 2.6 cm; length: 9.5 cm) was from Merck (Darmstadt, Germany). Amicon Ultra-15 Centrifugal Filter Units with 10,000-molecular-weight-cutoff were from Millipore (Billerica, MA, USA). Phosphoglucomutase from rabbit muscle (PGM) and glucose-6-phosphate dehydrogenase from *L. mesenteroides* (G6PDH) were from Sigma-Aldrich (Vienna, Austria). Glucose oxidase from *Aspergillus niger* (GOD), peroxidase from horseradish (POD) and 2,2′-azino-bis(3-ethylbenzothiazoline-6-sulfonic acid) diammonium salt (ABTS) were also from Sigma-Aldrich. The phosphonate analog of αGlc 1-*P* (2,6-anhydro-7-deoxy-7-phosphono-D-*glycero*-L-*gulo*-heptitol; herein: D-glucose 1-methylene phosphonate) was synthesized as previously described [20].

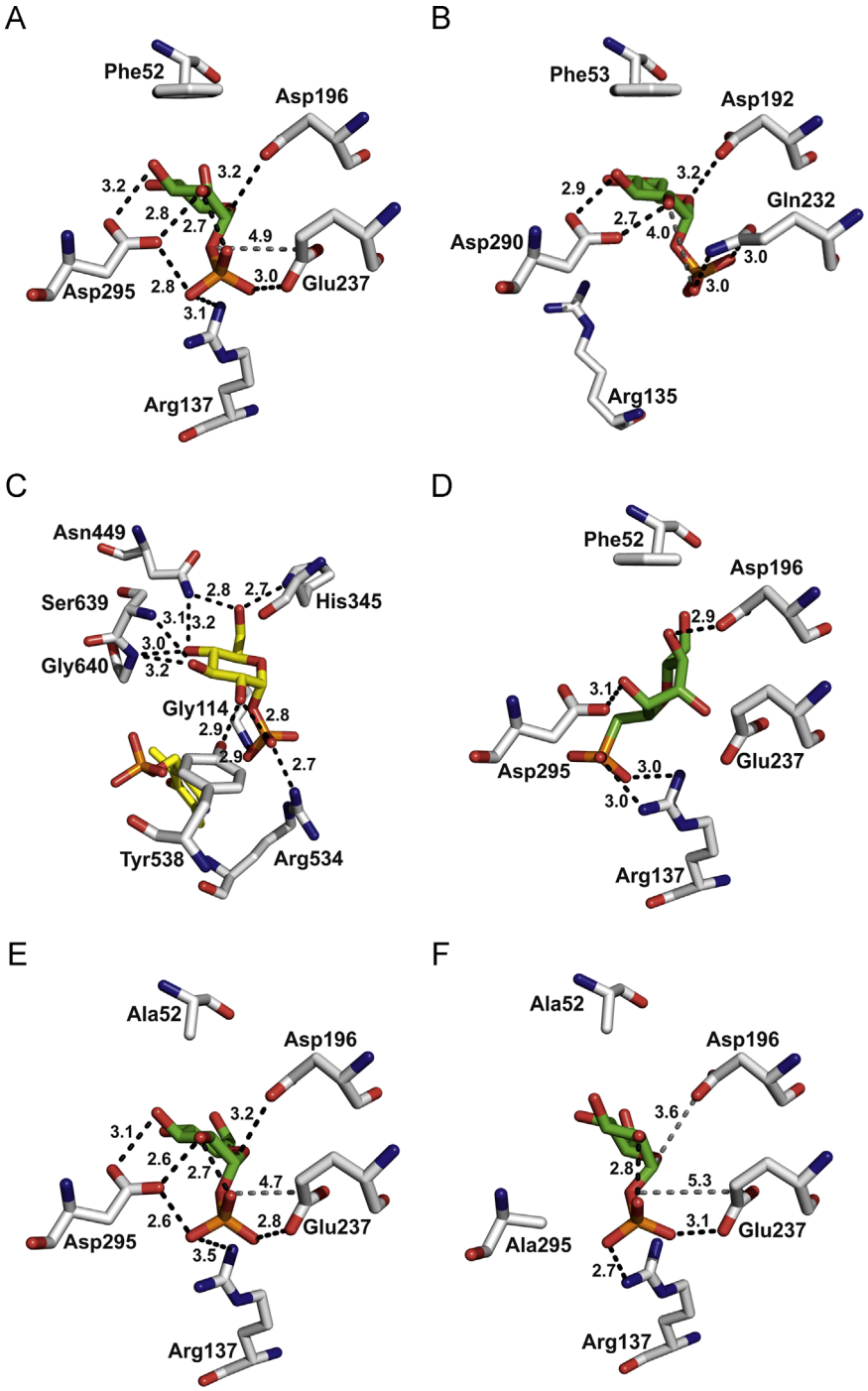

Fig. 1. Close-up views of the predicted binding of αGlc 1-*P* dianion at the catalytic site of sucrose phosphorylase. (A) Wild-type LmSPase (modeled). (B) E232N mutant of BaSPase (PDB entry 2gdu). (C) For reference, αGlc 1-*P* bound in maltodextrin phosphorylase from *E. coli* (PDB entry 1l5v). (D) D-Glucose 1-methylene phosphonate (dianion) binding to wild-type LmSPase. (E) F52A mutant. (F) F52A_D295A double mutant. Ligand carbon atoms are colored green, except for panel C where yellow color is used to highlight the different enzyme system. The pyridoxal 5′-phosphate cofactor of maltodextrin phosphorylase is also shown in panel C. Hydrogen bonds (≤ 3.5 Å) are shown as black-dashed lines. Interactions potentially relevant for catalysis are shown as gray-dashed lines. Distances are given in Å.

2.2. Site-directed mutagenesis, enzyme production and purification

The F52A variant of LmSPase was reported previously [11]. The F52A gene in pASK-IBA7+ expression vector was the template for introducing further mutation at Asp^{196}, Glu^{237} or Asp^{295} to generate F52A_D196A, F52A_E237A and F52A_D295A variants of the enzyme. The applied PCR was done exactly as described for creation of F52A variant [11], except that the annealing temperature was 47.6 °C for F52A_D196A and 61.8 °C for both F52A_E237A and F52A_D295A. The following mutagenic primers and their reverse complementary ones were used, whereby the mismatched bases are underlined:

F52A_D196A: 5′-ATTCGTTTGGCTGCCTTTGCG-3′;
F52A_E237A: 5′-CCATTAAAGGCTGAAATTTTACCAGCAATTCATG-3′;
F52A_D295A: 5′-GGACACGCATGCAGGTATTGGTG-3′.

Plasmid vectors harboring the verified mutated gene were transformed into electro-competent cells of *E. coli* BL21-Gold (DE3). Recipient strains were cultivated in 1-L baffeled shaken

flasks at 37 °C and 110 rpm using LB-media (200 mL) and 115 mg/L ampicillin. When OD_{550} reached 0.8–1.0, the temperature was decreased to 22 °C and gene expression was induced with 200 μg/L anhydrotetracycline for 20 h. Cells were centrifuged (4 °C, 5000 rpm, 30 min; Sorvall RC-5B Refrigerated Superspeed centrifuge; Du Pont Instruments, Wilmington, USA), resuspended in water and frozen at −20 °C. The thawed suspension was passed twice through a French pressure cell press (American Instruments, Silver Springs, USA) at 150 bar. Cell debris was removed by centrifugation (4 °C, 14,000 rpm, 30 min) and the resulting supernatant was used for enzyme purification.

A two-step purification procedure was used. Chromatography on *Strep*-Tactin Sepharose column was as described previously [22]. Pooled protein fractions were concentrated, loaded onto Fractogel EMD-DEAE and purified according to reported procedures [8]. Note that the second purification step was introduced after we noted that co-purification of phosphatase activity had occurred in some of the protein batches after the *Strep*-tag purification. The phosphatase hydrolyzed αGlc 1-*P* into D-glucose and phosphate and thus interfered with phosphorylase activity assays of weakly active LmSPase mutants. Phosphatase activity was completely absent in samples obtained via the two-step purification procedure. Buffer exchange to 50 mM MES (pH 7.0) was done using Amicon Ultra-15 Centrifugal Filter Units. Purification was monitored by SDS-PAGE.

2.3. Assays and analytical methods

A reported phosphorylase assay was used [11]. Briefly, enzyme activity for phosphorolysis of sucrose was determined at 30 °C in 50 mM MES (pH 7.0). Sucrose (100 mM) and phosphate (50 mM; sodium salt) were used a substrates. A continuous coupled assay with PGM and G6PDH was applied to determine the αGlc 1-*P* released in the enzymatic reaction. NADH produced in the coupled reaction is measured spectrophotometrically at 340 nm.

The following compounds were analyzed using protocols described previously [11,22]. Inorganic phosphate was measured colorimetrically at 850 nm (detection limit: 2.5 μM). D-Glucose was determined using a colorimetric GOD–POD assay (detection limit: 5 μM). αGlc 1-*P* and Glc 6-*P* were assayed enzymatically using PGM and G6PDH (detection limit: 50 μM). Sucrose synthesized in enzymatic reactions was measured using high performance anion exchange chromatography with pulsed amperometric detection (HPAE-PAD; detection limit of sucrose: 5 μM) [22]. Protein concentration was measured with the BioRad dye-binding method referenced against BSA.

2.4. Inhibition by D-glucose 1-methylene phosphonate

LmSPase catalyzes hydrolysis of αGlc 1-*P* under conditions where no acceptor substrate (e.g. D-fructose) is present in the reaction [2]. Enzyme was incubated with αGlc 1-*P* (5.0 mM) in the absence and presence of the phosphonate analog (5.0 mM). A 50 mM MES buffer (pH 7.0) was used. Release of phosphate was measured in regular intervals until a time of 50 min. In the case that the phosphonate analog competed with αGlc 1-*P* for binding to LmSPase, inhibition of the phosphate release rate was expected.

2.5. Chemical rescue studies

To potentially restore activity in F52A_E237A double mutant through "chemical rescue" effect [7], we supplied the enzymatic reaction mixture (10 mM αGlc 1-*P*, 0.3 mg/mL F52A_E237A, 50 mM MES, pH 7.0) with acetate, chloride, bromide, azide, cyanide or formate, each in a concentration of 50 mM of the sodium salt. The release of phosphate was measured over time for up to 24 h. Controls lacking the enzyme were used as reference.

2.6. Reaction with arsenate

Arsenolysis of αGlc 1-*P* is a reaction known to be catalyzed by LmSPase [2,7], where spontaneous decomposition of the formed α-D-glucose 1-arsenate results in release of D-glucose as the final reaction product. Incubations were done at 30 °C in 50 mM MES (pH 7.0) using 50 mM of each αGlc 1-*P* and sodium arsenate as substrates. F52A_E237A double mutant was present at 0.3 mg/mL. The D-glucose release was measured over time for up to 24 h. Controls lacking the enzyme were used as reference.

2.7. Initial-rate studies and steady-state kinetic analysis

Reactions were performed at 30 °C in 50 mM MES (pH 7.0) and monitored by product formation (phosphorolysis: αGlc 1-*P*; synthesis: phosphate) in discontinuous assays. Of the three double mutants prepared in this study, only the F52A_D295A exhibited an activity just sufficient for detailed kinetic analysis. Reactions were carried out at a protein concentration of 0.3 mg/mL and lasted for exactly 1 h. Donor or acceptor substrate was varied at 10–15 concentrations of sucrose (5.00–800 mM; 50 mM phosphate), phosphate (1.00–250 mM; 500 mM sucrose), αGlc 1-*P* (1.00–800 mM; 100 mM D-fructose) or D-fructose (0.01–100 mM; 20 mM αGlc 1-*P*). Control reactions lacking the substrate or the enzyme were recorded in all cases, and enzymatic rates were corrected for the blank readings as required. Kinetic parameters (V_{max}, K_m) were obtained for each half reaction in each direction of reaction (Scheme 1). Eq. (1) was fitted to initial-rate data obtained at variable substrate concentration. The difficulty of substrate inhibition by phosphate (Fig. S1, Supporting Information) was circumvented, by obtaining first estimates of kinetic parameters (V_{max}, K_m) from a Lineweaver–Burk plot. V_{max} and K_m were set constant and an estimate of the substrate inhibition constant K_i obtained from non-linear fits of Eq. (2) to the data. Refined estimates of V_{max} and K_m were obtained from non-linear fits of Eq. (2) using K_i as fixed parameter. Note: direct non-linear fit of Eq. (2) to the data whereby all three constants were used as fit parameters was not successful. Parameters showed high statistical correlation, rendering their independent determination impossible. The catalytic constant (k_{cat}) is defined in Eq. (3).

$$v = V_{max}S/(K_m + S) \quad (1)$$

$$v = V_{max}S/(K_m + S + S^2/K_i) \quad (2)$$

$$k_{cat} = V_{max}/E \quad (3)$$

In Eqs. (1)–(3), ν is the initial rate [mM/min], V_{max} is the maximum initial rate [mM/min], S is the substrate concentration [mM], K_m is the apparent Michaelis–Menten constant [mM], K_i is the substrate-inhibition constant [mM], k_{cat} is the catalytic constant [s^{-1}] and E is the total molar concentration of enzyme active-sites [mM], based on the protein concentration and molecular mass of 59 kDa for wild-type *Lm*SPase. When enzyme was not saturable with substrate and an independent determination of V_{max} and K_m therefore not possible, V_{max}/K_m was obtained from data acquired under substrate-limited reaction conditions where the rate increased linearly with substrate concentration.

2.8. Circular dichroism (CD) spectroscopy

Far-UV CD spectra of enzyme solutions (0.1 mg/mL; 50 mM MES, pH 7.0) were recorded at 22 °C on a Chirascan Plus system (Applied Photophysics, Leatherhead, UK) using quartz cuvette of

0.1 cm optical path. CD spectra were collected in the range 200–280 nm at a scan speed of 20 nm/min at 1.0 nm bandwidth and response time of 0.5 s. Each sample was measured five times. The resulting spectra were averaged and corrected with a buffer spectrum. CD signal was converted to molar ellipticity using the program CDNN [23].

2.9. Homology modeling and molecular docking

Homology models of LmSPase, F52A, F52A_D196A, F52A_E237A and F52A_D295A were built using SwissModel [24]. The structure of BaSPase E232Q mutant co-crystallized with sucrose (PDB entry 2gdu) [5] was manually selected as template. The structure of BaSPase wild-type bound with D-glucose (PDB entry 2gdv_B) was also used. AutoDock 4.2 [25] as implemented in Yasara V 11.11.21 was used for the enzyme-ligand docking. The AMBER03 force field [26] and the default parameters provided by the standard docking macro were used, except that the number of runs was increased to 50. Experimental structures of BaSPase or LmSPase homology models were used as macromolecules in a molecular docking experiment that employed αGlc 1-*P* mono- or dianion as ligand. 3D coordinates of the ligand were generated from SMILES strings using Chimera (http://www.cgl.ucsf.edu/chimera). The ligand was flexible placed into the macromolecule′s active-site. A search space of $15 \times 15 \times 25$ Å around the C1 atom of the catalytic nucleophile (LmSPase: Asp^{196}; BaSPase: Asp^{192}) was used. The same set-up was used to dock the phosphonate analog of αGlc 1-*P* into LmSPase. The docking algorithm typically resulted in 6 or more docking poses of similar free energy. We noted that while the position of the phosphate (phosphonate) group was almost identical in the different docking poses, the position of the D-glucopyranosyl ring was more strongly variable. The best-fit binding mode was therefore selected based on optimum structural alignment of the D-glucopyranosyl rings of the docked αGlc 1-*P* and the sucrose in the BaSPase crystal structure. PyMOL (http://pymol.sourceforge.net) was used for visualization.

2.10. Saturation transfer difference (STD) NMR

STD spectra were recorded as described earlier [27]. Samples were prepared in ^2H_2O (pH 6.65) and contained 50 mM MES, 7 μM enzyme and 5.0 mM ligand. Selective protein saturation was achieved by a series of 40 Gaussian pulses (50 ms length) with a 1 ms delay, resulting in a 2.04 s total irradiation time. On and off resonance irradiations were made by concomitant change of the irradiation frequencies at −2.0 ppm and 40.0 ppm, respectively. Each experiment was performed with two times 256 scan. A spin lock (30 ms) after the 90° pulse was used to eliminate the protein frequencies. No water suppression was applied to avoid influences of signals close to the HDO signal. Subtraction of the spectra was performed after the measurement. For the interpretation the largest signal in all comparable experiments was set to 100% and the relative intensities were determined in steps of 5% [27,28].

3. Results and discussion

3.1. Binding of αGlc 1-P examined with molecular docking

The best-fit docking pose for the αGlc 1-*P* dianion in LmSPase is shown in Fig. 1 (panel A). The αGlc 1-*P* was bound in an extended conformation that has the phosphate group positioned *anti* to the D-glucopyranosyl ring. The conformation adopted was very similar to the preferred conformation of αGlc 1-*P* in aqueous solution [29] whereby the D-glucopyranosyl ring was in a relaxed $^4C_1$ conformation. The relative position of the phosphate group corresponded to a specific rotamer around the C1–O bond where P was *trans* to C2. Intramolecular hydrogen bond between one phosphate O and the 2-OH was formed in the bound conformation of the αGlc 1-*P*.

Asp^{295} and Arg^{137} appeared to be highly important for recognition of the D-glucopyranosyl and phosphate groups of αGlc 1-*P*, respectively. Interestingly, Asp^{295} interacted mainly with the 2-OH and there was only a weak hydrogen bond with the 3-OH (Fig. 1, panel A). Asp^{196} was in a position that would allow it to perform nucleophilic attack on the anomeric center whereas Glu^{237} was in a position that would allow it to protonate the phosphate group. However, note that in the docking performed the sidechain of Glu^{237} was not protonated. Phe^{52} was positioned on top of the B-side of the D-glucopyranosyl ring, as required for its π cloud to function in transition state stabilization. Therefore, the docking pose in Fig. 1 (panel A) seemed to be a plausible representation of a catalytically productive binding mode of αGlc 1-*P*.

The docking pose of αGlc 1-*P* monoanion was almost superimposable on that of the dianion, except that the OH of the phosphate group now formed a hydrogen bond to Glu^{237} (Fig. S2). The docking pose of αGlc 1-*P* in BaSPase (E232Q mutant) which is shown in Fig. 1 (panel B) differed from that in LmSPase in that the phosphate group was positioned farther away from the D-glucopyranosylring, thus resulting in a somewhat stretched ligand conformation in which intramolecular hydrogen bonding between O_P and 2-OH was no longer possible. Phosphate was accommodated in BaSPase through interaction with the same active-site groups as in LmSPase, but the relative importance of these groups for phosphate binding was clearly different in the two docking poses. The phosphate moiety approached the uncharged Gln^{232} more closely than it approached the negatively charged Glu^{237} whereas concomitantly the phosphate distance to the arginine sidechain increased in E232Q_BaSPase as compared to LmSPase (Fig. 1, panels A and B). Docking of αGlc 1-*P* to a homology model of E237Q mutant of LmSPase (data not shown) gave essentially the same pose as in E232Q_BaSPase (Fig. 1, panel B), thus confirming the proposed effect of the site-directed substitution on the binding of the αGlc 1-*P* phosphate group. The E237Q mutant was previously reported to be just 9 times less efficient than the wild-type enzyme in catalyzing β-glucosylation of the sidechain of Asp^{196} from αGlc 1-*P* [7]. Therefore, this result might imply that both binding modes of αGlc 1-*P* in Fig. 1 are actually productive catalytically.

We also performed molecular docking of αGlc 1-*P* to another BaSPase structure (PDB entry 2gdv_B) that is a complex of the wild-type enzyme with β-D-glucose. The docking is shown in Fig. S3 (panel A). Aside from Glu^{232}, this wild-type structure [6] differs from the structure of E232Q mutant (PDB entry 2gdu) [6] in that, due to rearrangement of two loops lining the active-site, Arg^{135} adopts a slightly different position and Tyr^{344} swings into the catalytic center, switching position with Asp^{342} that interacted with the β-D-fructosyl group in the E232Q-sucrose complex structure [6]. Alanine mutagenesis of the corresponding residues in LmSPase (Asp^{338}, Tyr^{340}, Arg^{137}) revealed important roles of the arginine and the tyrosine in promoting specifically the enzymatic half-reaction with phosphate/αGlc 1-*P*. The Y340A mutant could no longer be saturated with phosphate or αGlc 1-*P*, suggesting that Tyr^{340} was important for binding of the phosphate group [10]. The homology model of LmSPase generated from BaSPase (PDB entry 2gdv_B) had Tyr^{340} and Arg^{137} in equivalent positions adopted by the template residues (Fig. S3, panel B). Interestingly, however, docking of αGlc 1-*P* to both enzyme structures yielded poses that were highly implausible catalytically (Fig. S3, panels A and B) and did not involve the tyrosine in the binding of the phosphate group. It is possible therefore that the BaSPase structure bound with

β-D-glucose (PDB entry 2gdv_B) does not represent the actual phosphate site of the enzyme and that induced fit-like rearrangements in active-site structure are still necessary to accommodate the phosphate group. Our modeling analysis was however not designed to examine effects of protein conformational flexibility and the role of Tyr^{340} was therefore not further pursued. Notwithstanding this, the evidence presented (Fig. 1, panels A and B) does suggest a plausible binding mode for αGlc 1-*P* that appears to be conducive to catalysis according to the proposed enzymatic mechanism (Scheme 1).

It is interesting to compare the conformation of αGlc 1-*P* in the phosphorylase docking poses with αGlc 1-*P* conformations in experimental structures of phosphorylases of another family type. Glycogen phosphorylase (PDB entry 3gpb) [30] and maltodextrin phosphorylase (PDB entry 1l5v) [18] accommodate their αGlc 1-*P* substrate in a highly similar conformation (Fig. 1, panel C) as the docking results suggest for SPase. This is noteworthy in particular because glycogen/maltodextrin phosphorylases are structurally (glycosyltransferase family GT-35) completely distinct from SPase (glycoside hydrolase family GH-13). The catalytic mechanism of glycogen/maltodextrin phosphorylases is also different from that of SPase. Enzymes from family GT-35 use a pyridoxal 5′-phosphate cofactor in catalysis and do not form a covalent glucosyl-enzyme intermediate in their reaction pathway. The binding pockets for αGlc 1-*P* are also different in SPase and glycogen/maltodextrin phosphorylase, as seen when comparing panels A and C in Fig. 1.

3.2. Binding of the phosphonate analog of αGlc 1-P

The D-glucose 1-methylene phosphonate [20] is a close structural analog of αGlc 1-*P* that does not have a scissile glycosidic bond and is therefore not a substrate of SPase. Note however that mimicry of αGlc 1-*P* is sufficient to enable the phosphonate to be used by some nucleotidyltransferases as alternative acceptor substrate instead of αGlc 1-*P* [20,21]. It was not expected therefore that the phosphonate analog did not even show inhibition of the LmSPase. Using conditions where αGlc 1-*P* was applied in limiting concentrations (5.0 mM) just around the K_m (4.7 mM), addition of the same concentration of phosphonate analog had no detectable effect on the rate of αGlc 1-*P* hydrolysis. The immediate suggestion of this result that the phosphonate analog did not bind to SPase under the conditions used was further examined by molecular docking as well as in STD-NMR studies.

Fig. 1 (panel D) shows the best-fit docking pose of the phosphonate analog. The predicted binding mode is totally different from that of αGlc 1-*P* and the calculated binding free energy is less favorable for the analog ($E = -4.6$ kcal/mol) as compared to αGlc 1-*P* ($E = -5.6$ kcal/mol). Fig. 2 summarizes the results of STD-NMR experiments. Binding of αGlc 1-*P* to LmSPase resulted in a characteristic pattern of STD effects that involved relatively strong interactions from the hydrogens at C6, C4 and C1. Due to overlap of signals from the MES buffer used, STD effects at C3 were not measurable. Just to note, the STD pattern of αGlc 1-*P* binding to a bacterial starch/maltodextrin phosphorylase from family GT-35 [31] was completely different from the one seen in LmSPase. Proximity of C-H hydrogens from αGlc 1-*P* to aliphatic or aromatic C–H hydrogens in LmSPase appears to explain the observable pattern of STD effects (Fig. 2). The D-glucose 1-methylene phosphonate did not give measurable STD effects on incubation with LmSPase, thus supporting the notion that binding of the phosphonate to the enzyme was very weak in comparison to the binding of αGlc 1-*P*.

3.3. Effects of site-directed substitutions in the active-site of LmSPase

Kinetic consequences of the site-directed replacement of Phe^{52} by Ala were reported in an earlier paper [11]. Fig. 1 (panel E) shows the docking pose of αGlc 1-*P* in a homology model of the F52A mutant. The bound αGlc 1-*P* adopted effectively the same conformation as in wild-type LmSPase. Interactions with residues of the active-site were also highly similar in the two docking poses (Fig. 1, panels A and E). The calculated αGlc 1-*P* binding energies were comparable for wild-type and F52A sucrose phosphorylases. The K_m for αGlc 1-*P* was previously shown to have decreased 12 times in F52A mutant (0.4 mM) as compared to wild-type enzyme, which appears to be consistent with the evidence from molecular docking (Fig. 1) insofar as the substitution of Phe^{52} by Ala did not disrupt the enzyme's affinity for binding αGlc 1-*P*. It is not possible from results of docking study or based on other evidence to explain why the K_m of αGlc 1-*P* is actually lower in the F52A mutant as compared to wild-type enzyme. One speculative possibility is that enzyme deglucosylation to fructose is even more strongly slowed down in F25A mutant compared to wild-type LmSPase than is enzyme glucosylation from αGlc 1-*P*. Therefore, this would result in accumulation of glucosyl enzyme intermediate at the steady-state and consequently a decrease in K_m. However, STD effects in αGlc 1-*P* were considerably weaker in F52A mutant than in wild-type enzyme and the relative distribution of STD effects across the glucosyl carbons was also slightly different for the F52A mutant (Fig. 2). Therefore, this strongly supports the suggestion from the docking studies that interactions with the phenyl ring of Phe^{52} are responsible for some of the STD effects that are produced in αGlc 1-*P* on its binding to the wild-type enzyme.

The double mutants F52A_D196A, F52A_E237A and F52A_D295A were obtained as highly purified enzyme preparations, as shown in Fig. S4. To verify proper folding of each mutant (including F52A) in comparison to the wild-type enzyme, a far-UV CD spectrum was recorded for each protein and processed with CDNN. Table S1 summarizes each enzyme's relative composition in secondary structural elements as calculated from the CD spectrum. There was no difference between wild-type and mutated enzymes above the error limit of the method used. The calculated relative distribution of α-helix and β-strand secondary structures was also in good agreement with the corresponding distributions in the homology model of LmSPase and the BaSPase crystal structure (α-helix: 37%; β-strand: 20%) [5,6]. Consequences of the site-directed substitutions are therefore analyzed with the assumption of correctly folded enzyme preparations.

The specific activity for phosphorolysis of sucrose was decreased 200-fold in F52A mutant (0.6 U/mg) as compared to wild-type enzyme (114 U/mg). The F52A_D295A double mutant had a specific activity of 0.4 U/mg, indicating that Asp^{295}-to-Ala substitution in the F52A mutant was by far less disruptive to the activity than was the single site-directed substitution of Asp^{295} by Asn in the wild-type enzyme. By way of comparison, the D295N mutant exhibited a specific activity of only 0.01 U/mg [9]. The F52A_D196A and F52A_E237A double mutants were not active above the detection limit of the used assay ($\geq 4 \times 10^{-4}$ U/mg). Relevant single-site mutants of LmSPase (D196A, E237N) were also inactive when assayed under analogous reaction conditions, as shown in earlier studies [7,8].

However, when tested for arsenolysis of αGlc 1-*P* where catalytic assistance from a general acid–base is not required for enzyme turnover to proceed effectively, the E237N mutant exhibited activity comparable to that of the wild-type LmSPase [7]. The F52A_E237A was therefore also examined for arsenolysis activity but did not show any above assay detection limit. Conversion of αGlc 1-*P* by the E237N mutant was stimulated (up to 300-fold) by different anions such as azide, which were shown to function as alternative glucosyl acceptor substrates that enhanced the turnover by speeding up the rate-limiting deglucosylation of the enzyme [7]. Various anions (azide, formate, acetate, bromide, chloride and

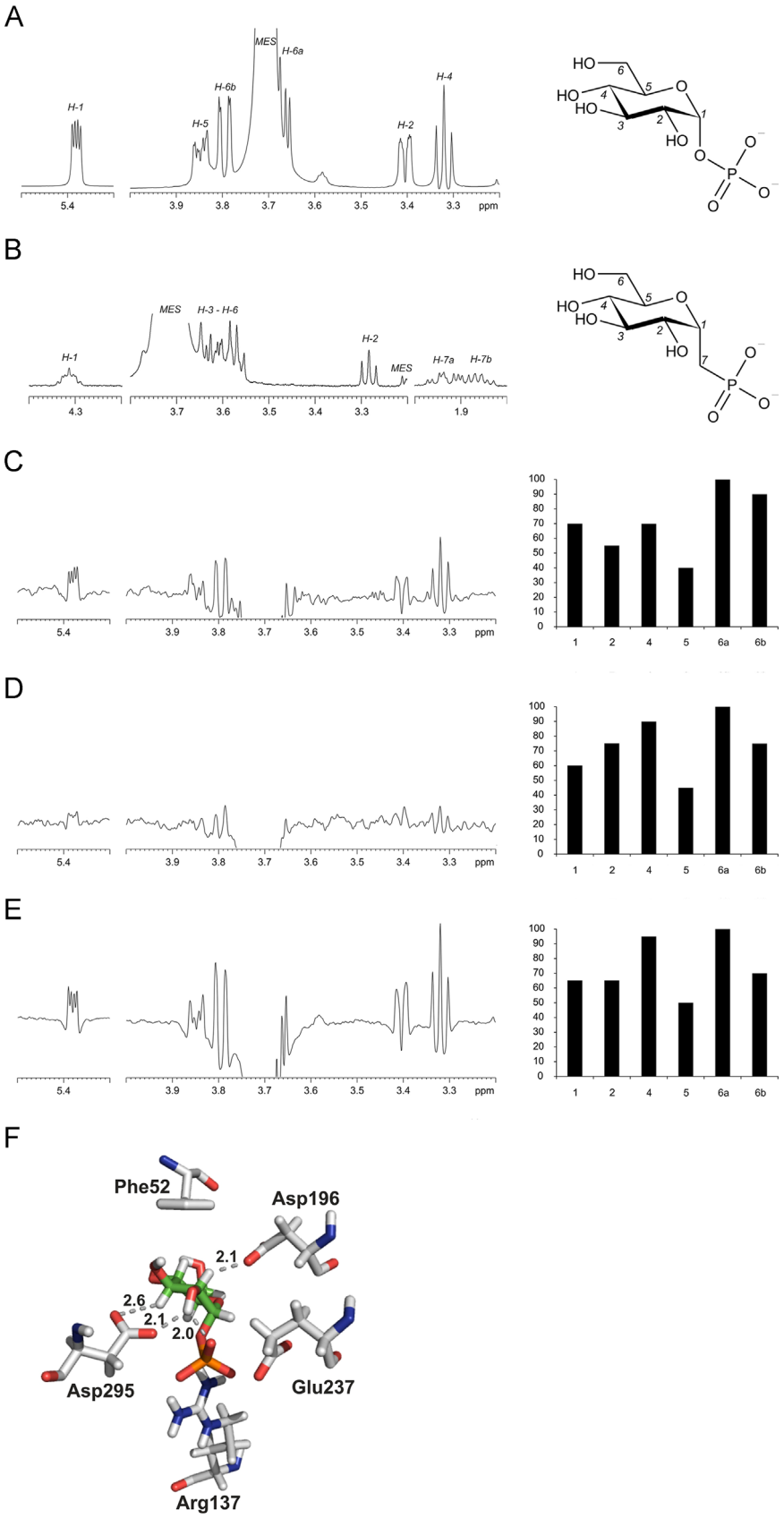

Fig. 2. Binding of αGlc 1-*P* to wild-type and mutated LmSPase characterized by STD-NMR. Each STD effect is the ratio of signal intensities in the STD spectrum and in the reference proton spectrum. STD effects are shown normalized on the largest effect in the sample. (A) ^{1}H NMR αGlc 1-*P*, (B) 1H NMR D-glucose 1-methylene phosphonate, (C) STD-NMR αGlc 1-*P*/wild-type LmSPase, (D) STD-NMR αGlc 1-*P*/F52A, (E) STD-NMR *α*Glc 1-*P*/F52A_D295A. (F) shows the molecular docking pose of *α*Glc 1-*P* in wild-type LmSPase to illustrate the vicinity of ligand C-H groups to aliphatic and aromatic hydrogens of the enzyme.

cyanide; each 50 mM) were also tested with the F52A_E237A mutant, but none was able to elicit activity.

Docking studies suggest that the additional mutation of Asp^{196} or Glu^{237} in an F52A mutant could affect the accommodation of αGlc 1-*P* in the enzyme's binding pocket to an extent that substrate positioning for reaction is no longer possible. The docking poses for F52A_D196A and F52A_E237A are shown in Fig. S5. Incubation of either double mutant with αGlc 1-*P* gave rise to distinct STD effects in the ligand, suggesting that binding of αGlc 1-*P* did take place in each double mutant, however, in a mode clearly different from that in wild-type enzyme or F52A mutant (Figs. 2 and S5).

3.4. Free-energy profile analysis for F52A_D295A double mutant

Detailed steady-state kinetic characterization of F52A_D295A double mutant was performed. The resulting kinetic parameters are summarized in Table S2 along with kinetic parameters of the wild-type enzyme, F52A [11] and D295N mutant [9] that were determined in earlier studies. The two-step reaction mechanism of LmSPase (Scheme 1) implies that the k_{cat}/K_m for glucosyl donor (sucrose, αGlc 1-*P*) and acceptor (phosphate, D-fructose) is the relevant kinetic expression for glucosylation and deglucosylation of Asp^{196} in the direction of phosphorolysis and synthesis, respectively. Fig. 3 compares the free-energy profiles constructed from the k_{cat}/K_m values assuming a 1 M standard state. Kinetic consequences in F52A_D295A mutant are discussed based on differences in free energy compared to the other phosphorylases.

Conversion of sucrose and phosphate into αGlc 1-*P* and D-fructose proceeds thermodynamically downhill ($\Delta\Delta G^{eq} = -1.3$ kcal/mol). In the wild-type enzyme, the covalent intermediate lies energetically exactly between the reactant and the product state. The transition states flanking the glucosyl enzyme intermediate present similar barriers ($\Delta\Delta G^{\#} \approx 11$–12 kcal/mol) to the catalytic reaction. Just like the single-site mutants F52A and D295N, the F52A_D295A double mutant featured pronounced destabilization ($\Delta\Delta G^{\#1} = 5.4$ kcal/mol) of the transition state of enzyme glucosylation from sucrose as compared to the wild-type enzyme. The second transition state was even more strongly destabilized ($\Delta\Delta G^{\#2} = 6.4$ kcal/mol) in the double mutant that was significantly less efficient in catalyzing enzyme glucosylation from αGlc 1-*P* than F25A mutant ($\Delta\Delta G^{\#2} = 3.5$ kcal/mol) and D295N mutant ($\Delta\Delta G^{\#2} = 5.6$ kcal/mol), in relation to wild-type LmSPase. Interestingly, while all other sucrose phosphorylases provided a similar amount of energetic stabilization to the β-glucosyl enzyme intermediate, the double mutant had clearly lost much of this ability ($\Delta\Delta G^{int} = 2.7$ kcal/mol). The double mutant was similar to previously characterized F52N and D295E single mutants in showing pronounced destabilization of the covalent enzyme intermediate.

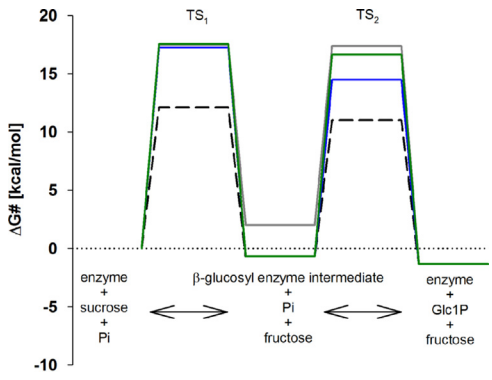

Fig. 3. Free-energy profile comparison for the catalytic reaction of F52A_D295A mutant (gray) with catalytic reactions of wild-type LmSPase (black dashed), F52A mutant (blue) and D295N (green) mutant. A standard state of 1 M was assumed. Kinetic parameters are from Table S2 in the Supporting Information. An equilibrium constant K_{eq} of 9 was used (pH 7.0, 30 °C). The free-energy profiles were constructed as described elsewhere [11]. Underlying equations are furthermore provided in Table S2.

The effects on $\Delta\Delta G^{int}$ encapsulated kinetic peculiarities of the F52A_D295A mutant (Table S2). Its apparent K_m of D-fructose was decreased 43-fold compared to the wild-type enzyme ($K_m = 13$ mM), despite the marked 130-fold loss in k_{cat}/K_m. The D295N mutant by contrast showed *elevated* K_m as compared to wild-type enzyme. The synthesis rate of F52A mutant was linearly dependent on the D-fructose concentration, so that K_m was not defined, however, strongly *decreased substrate binding affinity* was clearly indicated. Unlike wild-type and singly mutated enzymes, the F52A_D295A mutant showed substrate inhibition by phosphate ($K_i = 12$ mM). Plausible mechanism by which phosphate could cause inhibition is through binding to the free enzyme in competition with sucrose. However, more in-depth investigation of the substrate inhibition was beyond the scope of this study.

αGlc 1-*P* was docked into the F52A_D295A mutant and Fig. 1 (panel F) shows the best-fit binding mode. Compared to the docking poses for wild-type and F52A sucrose phosphorylases, the docking pose of F52A_D295A mutant had the position of D-glucopyranosylring slightly rotated whereas that of phosphate remained largely fixed through the interactions with Glu^{237} and Arg^{137}. It seems that the extra room created in the binding pocket of the double mutant allowed for binding of αGlc 1-*P* in a different orientation. Interestingly, hydrogen bond between O_P and 2-OH was still present. Distance of the αGlc 1-*P* anomeric carbon to Asp^{196} increased in the docking pose of F52A_D295A mutant as compared to the docking pose of the F25A mutant, apparently consistent with the lowered reactivity of the double mutant for enzyme glucosylation from αGlc 1-*P* (Fig. 3). STD effects in αGlc 1-*P* due to binding to the double mutant are summarized in Fig. 2. STD signal intensities were higher on binding of αGlc 1-*P* to F52A_D295A mutant as compared to wild-type and F52A sucrose phosphorylases. Reason for enhancement of the STD signals in the double mutant are not completely clear. Kinetic data show that the effect cannot be due to tighter apparent binding of αGlc 1-*P* by the double mutant as compared to wild-type enzyme or F52A mutant (Table S2). However, it must be considered that STD signal intensities not only reflect the strength of equilibrium binding, but also the *rates* of association and dissociation of the ligand. These rates are not directly accessible from the data presented in the paper. However, judging from the k_{cat}/K_m values for enzyme glucosylation from αGlc 1-*P* (Table S2), it is well possible that binding of αGlc 1-*P* was slowed down in the double mutant compared to wild-type enzyme and F52A mutant. This could have impacted the observable STD signals intensities. The pattern of relative STD effects obtained with F52A_D295A mutant was almost identical to that obtained with F52A mutant but differed from that of wild-type LmSPase (e.g. H2, H4, H6b).

4. Conclusions

Molecular docking studies suggest accommodation of αGlc 1-*P* in the active-site of sucrose phosphorylase in a conformation essentially identical to the conformation of αGlc 1-*P* bound in the structurally and mechanistically unrelated maltodextrin phosphorylase [19]. Both conformations of enzyme-bound αGlc 1-*P* are highly similar to the preferred conformation of αGlc 1-*P* in solution. The modeled conformation of αGlc 1-*P* bound in sucrose phosphorylase has the reactive groups of the substrate positioned relative to the catalytic groups of the enzyme such that reaction via β-glucosylation of Asp^{196} seems highly plausible. The inactive phosphonate analog of αGlc 1-*P* did not bind to sucrose

phosphorylase, consistent with the result of molecular docking that the best-fit binding mode of the analog was completely different from and energetically less favorable than the αGlc 1-*P* binding mode. Mutation of Phe^{52} into Ala did not affect the αGlc 1-*P* binding mode, consistent with the experimental result that the mutation had little effect on ground-state binding but resulted in selective destabilization of the transition states of the reaction [11]. Combining mutation of Phe^{52} with mutation of one of the catalytic triad residues was highly disruptive on αGlc 1-*P* binding and reactivity. Free-energy analysis of F52A_D295A mutant in relation to relevant free-energy profiles for wild-type and singly mutated sucrose phosphorylases suggest that Phe^{52} and Asp^{295} are together not only very important for transitions state stabilization, but they are also key for stabilization of the covalent β-glucosyl enzyme intermediate. These results appear to be of relevance not only for sucrose phosphorylase but also for other enzymes of the large glycoside hydrolase family GH-13.

Acknowledgments

Financial support from the Austrian Science Fund (FWF project L586-B03) is gratefully acknowledged. Can Araman (Institute of Biological Chemistry, University of Vienna, Austria) kindly helped in recording CD spectra.

Appendix A. Supporting information

Supporting data associated with this article can be found in the online version at http://dx.doi.org/10.1016/j.bbrep.2015.04.001.

Appendix B. Transparency document

Transparency document associated with this article can be found in the online version at http://dx.doi.org/10.1016/j.bbrep.2015.04.001.

References

[1] J.J. Mieyal, R.H. Abeles, Disaccharide phosphorylases, in: P.D. Boyer (Ed.), The Enzymes, 3rd ed.,Academic Press, New York, 1972, pp. 515–532.
[2] C. Luley-Goedl, B. Nidetzky, Biotechnol. J. 5 (2010) 1324–1338.
[3] E.A. MacGregor, S. Janecek, B. Svensson, Biochim. Biophys. Acta 9 (2001) 1–20.
[4] M. Stam, E.G.J. Danchin, C. Rancurel, P.M. Coutinho, B. Henrissat, Protein Eng. Des. Sel. 19 (2006) 555–562.
[5] O. Mirza, L.K. Skov, D. Sprogøe, L.A. van den Broek, G. Beldman, J.S. Kastrup, M. Gajhede, J. Biol. Chem. 281 (2006) 35576–35584.
[6] D. Sprogøe, L.A. van den Broek, O. Mirza, J.S. Kastrup, A.G. Voragen, M. Gajhede, L.K. Skov, Biochemistry 43 (2004) 1156–1162.
[7] A. Schwarz, L. Brecker, B. Nidetzky, Biochem. J. 403 (2007) 441–449.
[8] A. Schwarz, B. Nidetzky, FEBS Lett. 580 (2006) 3905–3910.
[9] M. Mueller, B. Nidetzky, FEBS Lett. 581 (2007) 1403–1408.
[10] M. Mueller, B. Nidetzky, FEBS Lett. 581 (2007) 3814–3818.
[11] P. Wildberger, C. Luley-Goedl, B. Nidetzky, FEBS Lett. 585 (2011) 499–504.
[12] M.H. Jensen, O. Mirza, C. Albenne, M. Remaud-Simeon, P. Monsan, M. Gajhede, L.K. Skov, Biochemistry 43 (2004) 3104–3110.
[13] M.I. Kim, H.S. Kim, J. Jung, S. Rhee, J. Mol. Biol. 380 (2008) 636–647.
[14] S. Ravaud, X. Robert, H. Watzlawick, R. Haser, R. Mattes, N. Aghajari, J. Biol. Chem. 282 (2007) 28126–28136.
[15] R. Renirie, A. Pukin, B. van Lagen, M.C.R. Franssen, J. Mol. Catal. B: Enzym. 67 (2010) 219–224.
[16] C. Goedl, A. Schwarz, A. Minani, B. Nidetzky, J. Biotechnol. 129 (2007) 77–86.
[17] D. Aerts, T.F. Verhaeghe, B. Roman, C.V. Stevens, T. Desmet, W. Soetaert, Carbohydr. Res. 346 (2011) 1860–1867.
[18] S. Kitao, H. Sekine, Biosci. Biotechnol. Biochem. 56 (1992) 2011–2014.
[19] S. Geremia, M. Campagnolo, R. Schinzel, L.N. Johnson, J. Mol. Biol. 322 (2002) 413–423.
[20] S.A. Beaton, M.P. Huestis, A. Sadeghi-Khomami, N.R. Thomas, D.L. Jakeman, Chem. Commun. (2009) 238–240.
[21] S.M. Forget, A. Jee, D.A. Smithen, R. Jagdhane, S. Anjum, S.A. Beaton, D.R.J. Palmer, R.T. Syvitski, D.L. Jakeman, Org. Biomol. Chem. 13 (2015) 866–875.
[22] P. Wildberger, A. Todea, B. Nidetzky, Biocatal. Biotransform. 30 (2012) 326–337.
[23] G. Bohm, R. Muhr, R. Jaenicke, Protein Eng. 5 (1992) 191–195.
[24] K. Arnold, L. Bordoli, J. Kopp, T. Schwede, Bioinformatics 22 (2006) 195–201.
[25] G.M. Morris, D.S. Goodsell, R.S. Halliday, R. Huey, W.E. Hart, R.K. Belew, A.J. Olson, J. Comput. Chem. 19 (1998) 1639–1662.
[26] Y. Duan, C. Wu, S. Chowdhury, M.C. Lee, G. Xiong, W. Zhang, R. Yang, P. Cieplak, R. Luo, T. Lee, J. Caldwell, J. Wang, P. Kollman, J. Comput. Chem. 24 (2003) 1999–2012.
[27] L. Brecker, G.D. Straganz, C.E. Tyl, W. Steiner, B. Nidetzky, J. Mol. Catal. B: Enzym. 42 (2006) 85–89.
[28] L. Brecker, A. Schwarz, C. Goedl, R. Kratzer, C.E. Tyl, B. Nidetzky, Carbohydr. Res. 343 (2008) 2153–2161.
[29] J.V. O'Connor, H.A. Nunez, R. Barker, Biochemistry 18 (1979) 500–507.
[30] J.L. Martin, L.N. Johnson, S.G. Withers, Biochemistry 29 (1990) 10745–10757.
[31] A. Schwarz, L. Brecker, B. Nidetzky, FEBS J. 274 (2007) 5105–5115.